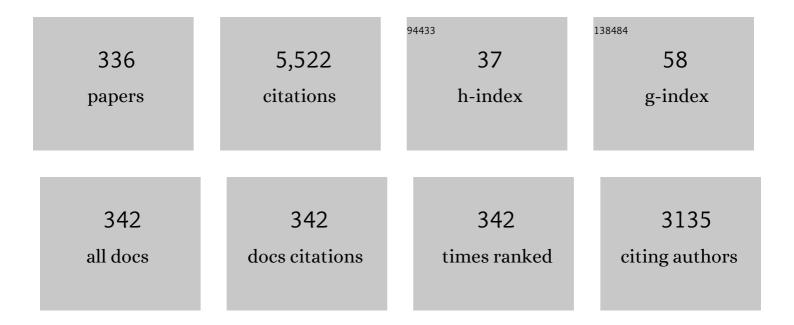
## Masaharu Shiratani

List of Publications by Year in descending order

Source: https://exaly.com/author-pdf/4360535/publications.pdf Version: 2024-02-01



#	Article	IF	CITATIONS
1	Morphological control of nanostructured Ge films in high Ar-gas-pressure plasma sputtering process for Li ion batteries. Japanese Journal of Applied Physics, 2022, 61, SA1002.	1.5	4
2	Improved luminescence performance of Yb3+-Er3+-Zn2+: Y2O3 phosphor and its application to solar cells. Optical Materials, 2022, 123, 111928.	3.6	4
3	Effect of gas flow rate and discharge volume on CO <sub>2</sub> methanation with plasma catalysis. Japanese Journal of Applied Physics, 2022, 61, SI1002.	1.5	7
4	Nanostructured Ge and GeSn films by high-pressure He plasma sputtering for high-capacity Li ion battery anodes. Scientific Reports, 2022, 12, 1742.	3.3	9
5	Outcomes of Pulsed Electric Fields and Nonthermal Plasma Treatments on Seed Germination and Protein Functions. Agronomy, 2022, 12, 482.	3.0	12
6	Growth of Single-Crystalline ZnO Films on 18%-Lattice-Mismatched Sapphire Substrates Using Buffer Layers with Three-Dimensional Islands. Crystal Growth and Design, 2022, 22, 3770-3777.	3.0	4
7	Effects of amplitude modulated capacitively coupled discharge Ar plasma on kinetic energy and angular distribution function of ions impinging on electrodes: particle-in-cell/Monte Carlo collision model simulation. Japanese Journal of Applied Physics, 2022, 61, 106003.	1.5	2
8	Mechanistic Insight into Permeation of Plasma-Generated Species from Vacuum into Water Bulk. International Journal of Molecular Sciences, 2022, 23, 6330.	4.1	5
9	Treatment of organic wastewater by a combination of non-thermal plasma and catalyst: a review. Reviews of Modern Plasma Physics, 2022, 6, .	4.1	11
10	Synthesis of Yb3+/Ho3+ co-doped Y2O3 nanoparticles and its application to dye sensitized solar cells. Journal of Molecular Structure, 2021, 1228, 129479.	3.6	12
11	Longâ€ŧerm response of Norway spruce to seed treatment with cold plasma: Dependence of the effects on the genotype. Plasma Processes and Polymers, 2021, 18, 2000159.	3.0	11
12	Impact of seed color and storage time on the radish seed germination and sprout growth in plasma agriculture. Scientific Reports, 2021, 11, 2539.	3.3	28
13	Possible impact of plasma oxidation on the structure of the C-terminal domain of SARS-CoV-2 spike protein: a computational study. Applied Physics Express, 2021, 14, 027002.	2.4	13
14	Green route for ammonium nitrate synthesis: fertilizer for plant growth enhancement. RSC Advances, 2021, 11, 28521-28529.	3.6	9
15	Alterations of DNA Methylation Caused by Cold Plasma Treatment Restore Delayed Germination of Heat-Stressed Rice ( <i>Oryza sativa</i> L.) Seeds. ACS Agricultural Science and Technology, 2021, 1, 5-10.	2.3	32
16	Impact of atmospheric pressure plasma treated seeds on germination, morphology, gene expression and biochemical responses. Japanese Journal of Applied Physics, 2021, 60, 040502.	1.5	24
17	Sputtering Growth of Metal Oxynitride Semiconductors for Excitonic Devices. , 2021, , .		0
18	Highly efficient and transparent counter electrode for application in bifacial solar cells. Chemical Physics Letters, 2021, 768, 138369.	2.6	6

#	Article	IF	CITATIONS
19	Comparison between Ar+CH4 cathode and anode coupling chemical vapor depositions of hydrogenated amorphous carbon films. Thin Solid Films, 2021, 729, 138701.	1.8	5
20	Plasma treatment causes structural modifications in lysozyme, and increases cytotoxicity towards cancer cells. International Journal of Biological Macromolecules, 2021, 182, 1724-1736.	7.5	21
21	Impact of Reactive Oxygen and Nitrogen Species Produced by Plasma on Mdm2–p53 Complex. International Journal of Molecular Sciences, 2021, 22, 9585.	4.1	5
22	Passivating antireflection coating of crystalline silicon using i/n a-Si:H/SiN trilayer. Journal of Physics and Chemistry of Solids, 2021, 156, 110127.	4.0	9
23	Effects of concentrated light on the performance and stability of a quasi-solid electrolyte in dye-sensitized solar cells. Chemical Physics Letters, 2021, 781, 138986.	2.6	5
24	Time of Flight Size Control of Carbon Nanoparticles Using Ar+CH4 Multi-Hollow Discharge Plasma Chemical Vapor Deposition Method. Processes, 2021, 9, 2.	2.8	5
25	Impact of surface morphologies of substrates on the epitaxial growth of magnetron-sputtered (ZnO) <i> <sub>x</sub> </i> (InN) <sub>1-<i>x</i> </sub> films. Japanese Journal of Applied Physics, 2021, 60, SAAB02.	1.5	3
26	Effect of hydrogen dilution on the silicon cluster volume fraction of a hydrogenated amorphous silicon film prepared using plasma-enhanced chemical vapor deposition. Current Applied Physics, 2020, 20, 191-195.	2.4	2
27	Relationship between cold plasma treatment-induced changes in radish seed germination and phytohormone balance. Japanese Journal of Applied Physics, 2020, 59, SH1001.	1.5	30
28	Real-time monitoring of surface passivation of crystalline silicon during growth of amorphous and epitaxial silicon layer. Journal of Applied Physics, 2020, 128, 033302.	2.5	8
29	Size and flux of carbon nanoparticles synthesized by Ar+CH4 multi-hollow plasma chemical vapor deposition. Diamond and Related Materials, 2020, 109, 108050.	3.9	14
30	Graphene-Si3N4 nanocomposite blended polymer counter electrode for low-cost dye-sensitized solar cells. Chemical Physics Letters, 2020, 758, 137920.	2.6	7
31	Plasma Agriculture from Laboratory to Farm: A Review. Processes, 2020, 8, 1002.	2.8	125
32	Cold Plasma Treatment of Sunflower Seeds Modulates Plant-Associated Microbiome and Stimulates Root and Lateral Organ Growth. Frontiers in Plant Science, 2020, 11, 568924.	3.6	20
33	Cold plasma treatment of <i>Arabidopsis thaliana</i> (L.) seeds modulates plant-associated microbiome composition. Applied Physics Express, 2020, 13, 076001.	2.4	13
34	Growth of single crystalline films on lattice-mismatched substrates through 3D to 2D mode transition. Scientific Reports, 2020, 10, 4669.	3.3	21
35	Characteristics of crystalline sputtered LaFeO <sub>3</sub> thin films as photoelectrochemical water splitting photocathodes. Nanoscale, 2020, 12, 9653-9660.	5.6	23
36	Improved Nanoscale Al-Doped ZnO with a ZnO Buffer Layer Fabricated by Nitrogen-Mediated Crystallization for Flexible Optoelectronic Devices. ACS Applied Nano Materials, 2020, 3, 2480-2490.	5.0	10

#	Article	IF	CITATIONS
37	Impact of radish sprouts seeds coat color on the electron paramagnetic resonance signals after plasma treatment. Japanese Journal of Applied Physics, 2020, 59, SHHF01.	1.5	20
38	Influence of osmolytes and ionic liquids on the Bacteriorhodopsin structure in the absence and presence of oxidative stress: A combined experimental and computational study. International Journal of Biological Macromolecules, 2020, 148, 657-665.	7.5	13
39	Effects of surrounding gas on plasma-induced downward liquid flow. Japanese Journal of Applied Physics, 2020, 59, SHHF02.	1.5	7
40	Influence of alkyl chain substitution of ammonium ionic liquids on the activity and stability of tobacco etch virus protease. International Journal of Biological Macromolecules, 2020, 155, 439-446.	7.5	8
41	Structural modification of NADPH oxidase activator (Noxa 1) by oxidative stress: An experimental and computational study. International Journal of Biological Macromolecules, 2020, 163, 2405-2414.	7.5	19
42	Plasma Treatment Effect on the Paramagnetic Species of Barley Seed Radical's Intensity: An EPR Study. Plasma Medicine, 2020, 10, 159-168.	0.6	4
43	Low-stress diamond-like carbon films containing carbon nanoparticles fabricated by combining rf sputtering and plasma chemical vapor deposition. Japanese Journal of Applied Physics, 2020, 59, 100906.	1.5	3
44	Experimental identification of the reactive oxygen species transported into a liquid by plasma irradiation. Japanese Journal of Applied Physics, 2020, 59, 110502.	1.5	8
45	Impact of heterointerface properties of crystalline germanium heterojunction solar cells. Thin Solid Films, 2019, 685, 225-233.	1.8	4
46	Effects of nitrogen impurity on zno crystal growth on Si substrates. MRS Advances, 2019, 4, 1557-1563.	0.9	0
47	Identification and Suppression of Si-H <sub>2 </sub> Bond Formation at P/I Interface in a-Si:H Films Deposited by SiH <sub>4 </sub> Plasma CVD. Plasma and Fusion Research, 2019, 14, 4406141-4406141.	0.7	1
48	Effects of Gas Pressure on the Size Distribution and Structure of Carbon Nanoparticles Using Ar + CH <sub>4 </sub> Multi-Hollow Discharged Plasma Chemical Vapor Deposition <sup> </sup> . Plasma and Fusion Research, 2019, 14, 4406115-4406115.	0.7	4
49	Dielectric barrier discharge plasma treatment-induced changes in sunflower seed germination, phytohormone balance, and seedling growth. Applied Physics Express, 2019, 12, 126003.	2.4	28
50	Local supply of reactive oxygen species into a tissue model by atmospheric-pressure plasma-jet exposure. Journal of Applied Physics, 2019, 125, 213303.	2.5	17
51	Sputter Epitaxy of (ZnO)x(InN)1-x films on Lattice-mismatched Sapphire Substrate. MRS Advances, 2019, 4, 1551-1556.	0.9	3
52	Visualization Study on Interaction Between Nonequilibrium Atmospheric Pressure He Plasma Jet and Liquid Solution. Journal of Smart Processing, 2019, 8, 58-63.	0.1	0
53	Spatial-Structure of Fluctuation of Amount of Nanoparticles in Amplitude-Modulated VHF Discharge Reactive Plasma. Plasma and Fusion Research, 2019, 14, 4406120-4406120.	0.7	2
54	Effect of Higher-Order Silane Deposition on Spatial Profile of Si-H <sub>2</sub> /Si-H Bond Density Ratio of a-Si:H Films. Plasma and Fusion Research, 2019, 14, 4406144-4406144.	0.7	0

#	Article	IF	CITATIONS
55	The effect of the H2/(H2 + Ar) flow-rate ratio on hydrogenated amorphous carbon films grown using Ar/H2/C7H8 plasma chemical vapor deposition. Thin Solid Films, 2018, 660, 891-898.	1.8	4
56	Impact of Gamma rays and DBD plasma treatments on wastewater treatment. Scientific Reports, 2018, 8, 2926.	3.3	49
57	Progress in photovoltaic performance of organic/inorganic hybrid solar cell based on optimal resistive Si and solvent modified poly(3,4â€ethylenedioxythiophene) poly(styrenesulfonate) junction. Progress in Photovoltaics: Research and Applications, 2018, 26, 145-150.	8.1	11
58	Current status and future prospects of agricultural applications using atmosphericâ€pressure plasma technologies. Plasma Processes and Polymers, 2018, 15, 1700073.	3.0	156
59	Transportation of reactive oxygen species in a tissue phantom after plasma irradiation. Japanese Journal of Applied Physics, 2018, 57, 01AG01.	1.5	6
60	Plasma agriculture: A rapidly emerging field. Plasma Processes and Polymers, 2018, 15, 1700174.	3.0	174
61	Effects of Sputtering Pressure on (ZnO) <sub>x</sub> (InN) <sub>1-x</sub> Crystal Film Growth at 450°C. Materials Science Forum, 2018, 941, 2093-2098.	0.3	0
62	Cross-Correlation Analysis of Fluctuations of Interactions between Nanoparticles and Low Pressure Reactive Plasmas. Materials Science Forum, 2018, 941, 2104-2108.	0.3	0
63	Morphology Evolution Of ZnO Thin Films Deposited By Nitrogen Mediated Crystallization Method. MATEC Web of Conferences, 2018, 159, 02031.	0.2	3
64	Particle behavior and its contribution to film growth in a remote silane plasma. Journal of Vacuum Science and Technology A: Vacuum, Surfaces and Films, 2018, 36, 050601.	2.1	1
65	Dependence of CO <sub>2</sub> Conversion to CH <sub>4 </sub> on the CO <sub>2</sub> Flow Rate in a Helicon Discharge Plasma. Science of Advanced Materials, 2018, 10, 655-659.	0.7	4
66	Low-Pressure Methanation of CO <sub>2</sub> Using a Plasma–Catalyst System. Science of Advanced Materials, 2018, 10, 1087-1090.	0.7	5
67	Effects of Gas Velocity on Deposition Rate and Amount of Cluster Incorporation into a-Si:H Films Fabricated by SiH <sub>4 </sub> Plasma Chemical Vapor Deposition. Plasma and Fusion Research, 2018, 13, 1406082-1406082.	0.7	5
68	Hysteresis in volume fraction of clusters incorporated into a-Si:H films deposited by SiH 4 plasma chemical vapor deposition. Surface and Coatings Technology, 2017, 326, 388-394.	4.8	6
69	Densities and Surface Reaction Probabilities of Oxygen and Nitrogen Atoms During Sputter Deposition of ZnInON on ZnO. IEEE Transactions on Plasma Science, 2017, 45, 323-327.	1.3	11
70	Enhanced light harvesting and charge recombination control with TiO2/PbCdS/CdS based quantum dot-sensitized solar cells. Journal of Electroanalytical Chemistry, 2017, 788, 131-136.	3.8	24
71	Plant Growth Enhancement of Seeds Immersed in Plasma Activated Water. MRS Advances, 2017, 2, 995-1000.	0.9	38
72	Synthesis of Nanoparticles Using Low Temperature Plasmas and Its Application to Solar Cells and Tracers in Living Body. ECS Transactions, 2017, 77, 17-24.	0.5	0

#	Article	IF	CITATIONS
73	Low temperature rapid formation of Au-induced crystalline Ge films using sputtering deposition. Thin Solid Films, 2017, 641, 59-64.	1.8	5
74	Effects of sputtering gas pressure dependence of surface morphology of ZnO films fabricated via nitrogen mediated crystallization. MRS Advances, 2017, 2, 265-270.	0.9	4
75	Blue Photoluminescence of (ZnO)0.92(InN)0.08. MRS Advances, 2017, 2, 277-282.	0.9	8
76	The protective action of osmolytes on the deleterious effects of gamma rays and atmospheric pressure plasma on protein conformational changes. Scientific Reports, 2017, 7, 8698.	3.3	19
77	Impact of an ionic liquid on protein thermodynamics in the presence of cold atmospheric plasma and gamma rays. Physical Chemistry Chemical Physics, 2017, 19, 25277-25288.	2.8	19
78	Performance enhancement of quantum dot-sensitized solar cells based on polymer nano-composite catalyst. Electrochimica Acta, 2017, 249, 337-342.	5.2	2
79	Biogenic reductive preparation of magnetic inverse spinel iron oxide nanoparticles for the adsorption removal of heavy metals. Chemical Engineering Journal, 2017, 307, 74-84.	12.7	226
80	Response of Silkworm Larvae to Atmospheric Pressure Nonthermal Plasma Irradiation. Plasma Medicine, 2016, 6, 349-359.	0.6	1
81	DNA Microarray Analysis of Plant Seeds Irradiated by Active Oxygen Species in Oxygen Plasma. Plasma Medicine, 2016, 6, 459-471.	0.6	15
82	Effect of sulfur doped TiO2 on photovoltaic properties of dye-sensitized solar cells. Electronic Materials Letters, 2016, 12, 530-536.	2.2	13
83	Inter-particle potential fluctuation of two fine particles suspended in Ar plasmas. , 2016, , .		Ο
84	Correlation between SiH <sub>2</sub> /SiH and light-induced degradation of p–i–n hydrogenated amorphous silicon solar cells. Japanese Journal of Applied Physics, 2016, 55, 07LE03.	1.5	8
85	Effects of nonthermal plasma jet irradiation on the selective production of H2O2 and NO2â^' in liquid water. Journal of Applied Physics, 2016, 120, .	2.5	52
86	Fluctuation of Position and Energy of a Fine Particle in Plasma Nanofabrication. Materials Science Forum, 2016, 879, 1772-1777.	0.3	5
87	Two-dimensional concentration distribution of reactive oxygen species transported through a tissue phantom by atmospheric-pressure plasma-jet irradiation. Applied Physics Express, 2016, 9, 076202.	2.4	41
88	Effects of irradiation distance on supply of reactive oxygen species to the bottom of a Petri dish filled with liquid by an atmospheric O2/He plasma jet. Journal of Applied Physics, 2016, 119, .	2.5	36
89	Low temperature synthesis of silicon quantum dots with plasma chemistry control in dual frequency non-thermal plasmas. Physical Chemistry Chemical Physics, 2016, 18, 15697-15710.	2.8	16
90	Room Temperature Fabrication of (ZnO)x(InN)1-x films with Step-Terrace Structure by RF Magnetron Sputtering. MRS Advances, 2016, 1, 115-119.	0.9	9

#	Article	IF	CITATIONS
91	Improving the performance of quantum dot sensitized solar cells through CdNiS quantum dots with reduced recombination and enhanced electron lifetime. Dalton Transactions, 2016, 45, 8447-8457.	3.3	44
92	Optical Bandgap Energy of Si Nanoparticle Composite Films Deposited by a Multi-Hollow Discharge Plasma Chemical Vapor Deposition Method. Journal of Nanoscience and Nanotechnology, 2016, 16, 10753-10757.	0.9	2
93	Variation in structure of proteins by adjusting reactive oxygen and nitrogen species generated from dielectric barrier discharge jet. Scientific Reports, 2016, 6, 35883.	3.3	40
94	Mechanism and comparison of needle-type non-thermal direct and indirect atmospheric pressure plasma jets on the degradation of dyes. Scientific Reports, 2016, 6, 34419.	3.3	71
95	Production of In, Au, and Pt nanoparticles by discharge plasmas in water for assessment of their bio-compatibility and toxicity. MRS Advances, 2016, 1, 1301-1306.	0.9	0
96	Relationship between electric properties and surface flatness of (ZnO) <inf>x</inf> (InN) <inf>1â^'x</inf> films on ZnO templates. , 2016, , .		0
97	Plant Growth Response to Atmospheric Air Plasma Treatments of Seeds of 5 Plant Species. MRS Advances, 2016, 1, 1265-1269.	0.9	9
98	Surface Modification of Polymer Counter Electrode for Low Cost Dye-sensitized Solar Cells. Electrochimica Acta, 2016, 210, 880-887.	5.2	12
99	Catalytic Improvement on Counter Electrode of Dye-Sensitized Solar Cells Using Electrospun Pt Nano-Fibers. Journal of Nanoscience and Nanotechnology, 2016, 16, 3332-3337.	0.9	1
100	Effects of plasma irradiation using various feeding gases on growth of Raphanus sativus L. Archives of Biochemistry and Biophysics, 2016, 605, 129-140.	3.0	64
101	Improvement of Charge Transportation in Si Quantum Dot-Sensitized Solar Cells Using Vanadium Doped TiO <sub>2</sub> . Journal of Nanoscience and Nanotechnology, 2016, 16, 4875-4879.	0.9	4
102	Effects of gas flow rate on deposition rate and number of Si clusters incorporated into a-Si:H films. Japanese Journal of Applied Physics, 2016, 55, 01AA19.	1.5	5
103	Reduced recombination with an optimized barrier layer on TiO <sub>2</sub> in PbS/CdS core shell quantum dot sensitized solar cells. New Journal of Chemistry, 2016, 40, 3423-3431.	2.8	23
104	Simple method of improving harvest by nonthermal air plasma irradiation of seeds of Arabidopsis thaliana (L.). Applied Physics Express, 2016, 9, 016201.	2.4	83
105	Polymer counter electrode of poly(3,4-ethylenedioxythiophene):Poly(4-styrenesulfonate) containing TiO2 nano-particles for dye-sensitized solar cells. Journal of Power Sources, 2016, 307, 25-30.	7.8	32
106	Quantum Characterization of Si Nano-Particles Fabricated by Multi-Hollow Discharge Plasma Chemical Vapor Deposition. Science of Advanced Materials, 2016, 8, 636-639.	0.7	1
107	Effects of deposition rate and ion bombardment on properties of a-C:H films deposited by H-assisted plasma CVD method. Japanese Journal of Applied Physics, 2016, 55, 01AA11.	1.5	9
108	Fabrication of p-i-n solar cells utilizing ZnInON by RF magnetron sputtering. Materials Research Society Symposia Proceedings, 2015, 1741, 53.	0.1	3

#	Article	IF	CITATIONS
109	Antioxidative activity and growth regulation of Brassicaceae induced by oxygen radical irradiation. Japanese Journal of Applied Physics, 2015, 54, 06GD01.	1.5	40
110	Effects of gas flow on oxidation reaction in liquid induced by He/O2 plasma-jet irradiation. Journal of Applied Physics, 2015, 118, .	2.5	39
111	Influence of ionic liquid and ionic salt on protein against the reactive species generated using dielectric barrier discharge plasma. Scientific Reports, 2015, 5, 17781.	3.3	70
112	Deposition of Germanium Crystalline Nanoparticle Composite Films by Using Reactive Dusty Plasma Process and their Application for Quantum-Dot Solar Cells. Journal of Smart Processing, 2015, 4, 6-11.	0.1	0
113	Effects of Atmospheric Air Plasma Irradiation to Seeds of Radish Sprouts on Chlorophyll and Carotenoids Concentrations in their Leaves. Materials Research Society Symposia Proceedings, 2015, 1723, 34.	0.1	4
114	Effects of morphology of buffer layers on ZnO/sapphire heteroepitaxial growth by RF magnetron sputtering. Materials Research Society Symposia Proceedings, 2015, 1741, 33.	0.1	4
115	Comparative Study on the Pulmonary Toxicity of Indium Hydroxide, Indium-Tin Oxide, and Indium Oxide Following Intratracheal Instillations into the Lungs of Rats. Materials Research Society Symposia Proceedings, 2015, 1723, 19.	0.1	Ο
116	Fabrication of ZnInON/ZnO multi-quantum well solar cells. Thin Solid Films, 2015, 587, 106-111.	1.8	15
117	Real-time mass measurement of dust particles deposited on vessel wall in a divertor simulator using quartz crystal microbalances. Journal of Nuclear Materials, 2015, 463, 865-868.	2.7	2
118	Synthesis of Indium-Containing Nanoparticles in Aqueous Suspension Using Plasmas in Water for Evaluating Their Kinetics in Living Body. Journal of Nanoscience and Nanotechnology, 2015, 15, 9298-9302.	0.9	1
119	Effects of cluster incorporation into hydrogenated amorphous silicon films in initial discharge phase on film stability. Thin Solid Films, 2015, 587, 126-131.	1.8	10
120	Multigeneration Effects of Plasma Irradiation to Seeds of Arabidopsis Thaliana and Zinnia on Their Growth. Materials Research Society Symposia Proceedings, 2015, 1723, 7.	0.1	7
121	Photovoltaic application of Si nanoparticles fabricated by multihollow plasma discharge CVD: Dye and Si co-sensitized solar cells. Japanese Journal of Applied Physics, 2015, 54, 01AD02.	1.5	4
122	Structural alternation of tandem dye-sensitized solar cells based on mesh-type of counter electrode. Electrochimica Acta, 2015, 179, 206-210.	5.2	4
123	Gas Flow Rate Dependence of the Discharge Characteristics of a Plasma Jet Impinging Onto the Liquid Surface. IEEE Transactions on Plasma Science, 2015, 43, 4081-4087.	1.3	13
124	Deposition of Carbon Films on PMMA Using H-assisted Plasma CVD. , 2014, , .		0
125	Growth mechanism of ZnO deposited by nitrogen mediated crystallization. Materials Research Express, 2014, 1, 036403.	1.6	6
126	Self-organized formation of hierarchically-ordered structures in laser-activated plasma CVD of sp3-bonded BN films. Japanese Journal of Applied Physics, 2014, 53, 010202.	1.5	1

#	Article	IF	CITATIONS
127	Formation of microcones accompanied with ripple patterns in laser-activated plasma CVD of <i>sp</i> <sup>3</sup> -bonded BN films. Journal of Materials Research, 2014, 29, 485-491.	2.6	Ο
128	Sterilization characteristics of the surfaces of agricultural products using active oxygen species generated by atmospheric plasma and UV light. Japanese Journal of Applied Physics, 2014, 53, 05FR03.	1.5	30
129	Off-axis sputter deposition of ZnO films on c-sapphire substrates by utilizing nitrogen-mediated crystallization method. Optical Engineering, 2014, 53, 087109.	1.0	10
130	Study on the Crystal Growth Mechanism of ZnO Films Fabricated Via Nitrogen Mediated Crystallization , 2014, , .		0
131	Performance dependence of Si quantum dot-sensitized solar cells on counter electrode. Japanese Journal of Applied Physics, 2014, 53, 05FZ01.	1.5	4
132	SiC Nanoparticle Composite Anode for Li-Ion Batteries. Materials Research Society Symposia Proceedings, 2014, 1678, 7.	0.1	7
133	Electrochemical impedance analysis on the additional layers for the enhancement on the performance of dye-sensitized solar cell. Thin Solid Films, 2014, 554, 122-126.	1.8	7
134	Plasma induced long-term growth enhancement of Raphanus sativus L. using combinatorial atmospheric air dielectric barrier discharge plasmas. Current Applied Physics, 2014, 14, S149-S153.	2.4	85
135	Analysis on the photovoltaic property of Si quantum dot-sensitized solar cells. International Journal of Precision Engineering and Manufacturing, 2014, 15, 339-343.	2.2	5
136	Effects of Atmospheric Air Plasma Irradiation on pH of Water. , 2014, , .		3
137	Dust Hour Glass in a Capacitive RF Discharge. IEEE Transactions on Plasma Science, 2014, 42, 2672-2673.	1.3	2
138	Visualization of the Distribution of Oxidizing Substances in an Atmospheric Pressure Plasma Jet. IEEE Transactions on Plasma Science, 2014, 42, 2482-2483.	1.3	30
139	Theory for correlation between plasma fluctuation and fluctuation of nanoparticle growth in reactive plasmas. Japanese Journal of Applied Physics, 2014, 53, 010201.	1.5	9
140	The enhancement of dye adsorption in dye-sensitized solar module by an electrical adsorption method. Thin Solid Films, 2014, 554, 118-121.	1.8	7
141	Effects of Grid DC Bias on Incorporation of Si Clusters into Amorphous Silicon Thin Films in Multi-Hollow Discharge Plasma CVD. , 2014, , .		0
142	Performance enhancement of dye and Si quantum dot hybrid nanostructured solar cell with TiO <sub>2</sub> barrier. Transactions of the Materials Research Society of Japan, 2014, 39, 321-324.	0.2	0
143	Effects of H2 Gas Addition on Structure of Ge Nanoparticle Films Deposited by High-Pressure RF Magnetron Sputtering Method. , 2014, , .		0
144	Combinatorial Plasma CVD of Si Nanoparticle Composite Films for Band Gap Control. , 2014, , .		0

#	Article	IF	CITATIONS
145	Mass density control of carbon films deposited by H-assisted plasma CVD method. Surface and Coatings Technology, 2013, 228, S15-S18.	4.8	9
146	Transport control of dust particles via the electrical asymmetry effect: experiment, simulation and modelling. Journal Physics D: Applied Physics, 2013, 46, 245202.	2.8	16
147	Growth control of ZnO nano-rod with various seeds and photovoltaic application. Journal of Physics: Conference Series, 2013, 441, 012029.	0.4	1
148	Analysis on the effect of polysulfide electrolyte composition for higher performance of Si quantum dot-sensitized solar cells. Electrochimica Acta, 2013, 95, 43-47.	5.2	31
149	Characteristics of photocurrent generation in the near-ultraviolet region in Si quantum-dot sensitized solar cells. Thin Solid Films, 2013, 544, 93-98.	1.8	10
150	The improvement on the performance of quantum dot-sensitized solar cells with functionalized Si. Thin Solid Films, 2013, 546, 284-288.	1.8	6
151	Effects of nanoparticle incorporation on properties of microcrystalline films deposited using multi-hollow discharge plasma CVD. Surface and Coatings Technology, 2013, 228, S550-S553.	4.8	1
152	Discharge power dependence of carbon dust flux in a divertor simulator. Journal of Nuclear Materials, 2013, 438, S788-S791.	2.7	5
153	The reduction of charge recombination and performance enhancement by the surface modification of Si quantum dot-sensitized solar cell. Electrochimica Acta, 2013, 87, 213-217.	5.2	18
154	Effects of DC substrate bias voltage on dust flux in the Large Helical Device. Journal of Nuclear Materials, 2013, 438, S727-S730.	2.7	5
155	Dust particle formation due to interaction between graphite and helicon deuterium plasmas. Fusion Engineering and Design, 2013, 88, 28-32.	1.9	10
156	Plasma interactions with aminoacid (l-alanine) as a basis of fundamental processes in plasma medicine. Current Applied Physics, 2013, 13, S59-S63.	2.4	22
157	High Amount Cluster Incorporation in Initial Si Film Deposition by SiH4Plasma Chemical Vapor Deposition. Japanese Journal of Applied Physics, 2013, 52, 01AD01.	1.5	12
158	H2/N2Plasma Etching Rate of Carbon Films Deposited by H-Assisted Plasma Chemical Vapor Deposition. Japanese Journal of Applied Physics, 2013, 52, 01AB01.	1.5	3
159	Correlation between Volume Fraction of Silicon Clusters in Amorphous Silicon Films and Optical Emission Properties of Si <sup>*</sup> and SiH <sup>*</sup> . Japanese Journal of Applied Physics, 2013, 52, 11NA07.	1.5	4
160	Improvement of Si Adhesion and Reduction of Electron Recombination for Si Quantum Dot-Sensitized Solar Cells. Japanese Journal of Applied Physics, 2013, 52, 01AD05.	1.5	12
161	Flux Control of Carbon Nanoparticles Generated due to Interactions between Hydrogen Plasmas and Graphite Using DC-Biased Substrates. Japanese Journal of Applied Physics, 2013, 52, 11NA08.	1.5	2
162	Characteristics of Crystalline Silicon/Si Quantum Dot/Poly(3,4-ethylenedioxythiophene) Hybrid Solar Cells. Japanese Journal of Applied Physics, 2013, 52, 11NA05.	1.5	1

#	Article	IF	CITATIONS
163	Effects of Nitrogen on Crystal Growth of Sputter-Deposited ZnO Films for Transparent Conducting Oxide. Japanese Journal of Applied Physics, 2013, 52, 11NB03.	1.5	14
164	Improvement on the Electron Transfer of Dye-Sensitized Solar Cell Using Vanadium Doped TiO <sub>2</sub> . Japanese Journal of Applied Physics, 2013, 52, 11NM02.	1.5	11
165	Epitaxial Growth of ZnInON Films with Tunable Band Gap from 1.7 to 3.3 eV on ZnO Templates. Japanese Journal of Applied Physics, 2013, 52, 11NM06.	1.5	16
166	Study on the Fabrication of Paint-Type Si Quantum Dot-Sensitized Solar Cells. Japanese Journal of Applied Physics, 2013, 52, 10MB07.	1.5	7
167	Effects of Hydrogen Dilution on ZnO Thin Films Fabricated via Nitrogen-Mediated Crystallization. Japanese Journal of Applied Physics, 2013, 52, 01AC08.	1.5	9
168	Investigations on Plasma-Biomolecules Interactions as Fundamental Process for Plasma Medicine. Journal of Physics: Conference Series, 2013, 441, 012001.	0.4	7
169	Research Productivity Enhancement. Hyomen Kagaku, 2013, 34, 519-519.	0.0	0
170	The Optical Analysis and Application of Size-controllable Si Quantum Dots Fabricated by Multi-hollow Discharge Plasma Chemical Vapor Deposition. Materials Research Society Symposia Proceedings, 2012, 1426, 313-318.	0.1	0
171	Influence of Atmospheric Pressure Torch Plasma Irradiation on Plant Growth. Materials Research Society Symposia Proceedings, 2012, 1469, 92.	0.1	4
172	Rapid Growth of Radish Sprouts Using Low Pressure O <sub>2</sub> Radio Frequency Plasma Irradiation. Materials Research Society Symposia Proceedings, 2012, 1469, 61.	0.1	4
173	Characteristics of stable a-Si:H Schottoky cells fabricated by suppressing cluster deposition. Materials Research Society Symposia Proceedings, 2012, 1426, 377-382.	0.1	1
174	Combinatorial Deposition of Microcrystalline Silicon Films Using Multihollow Discharge Plasma Chemical Vapor Deposition. Japanese Journal of Applied Physics, 2012, 51, 01AD02.	1.5	3
175	Effect of Nitridation of Si Nanoparticles on the Performance of Quantum-Dot Sensitized Solar Cells. Japanese Journal of Applied Physics, 2012, 51, 01AD01.	1.5	7
176	Deposition of Cluster-Free B-doped Hydrogenated Amorphous Silicon Films Using SiH\$_{4}\$+B\$_{10}\$H\$_{14}\$ Multi-Hollow Discharge Plasma Chemical Vapor Deposition. Japanese Journal of Applied Physics, 2012, 51, 01AD03.	1.5	2
177	Effects of Irradiation with Ions and Photons in Ultraviolet–Vacuum Ultraviolet Regions on Nano-Surface Properties of Polymers Exposed to Plasmas. Japanese Journal of Applied Physics, 2012, 51, 01AJ02.	1.5	1
178	Improvement on the Long-Term Stability of Dye-Sensitized Solar Module by Structural Alternation. Japanese Journal of Applied Physics, 2012, 51, 10NE21.	1.5	2
179	Impacts of plasma fluctuation on nanoparticle growth in reactive plasmas. , 2012, , .		0
180	Growth Enhancement of Radish Sprouts Induced by Low Pressure O <sub>2</sub> Radio Frequency Discharge Plasma Irradiation. Japanese Journal of Applied Physics, 2012, 51, 01AE01.	1.5	32

#	Article	IF	CITATIONS
181	In-situ Measurements of Cluster Volume Fraction in Silicon Thin Films Using Quartz Crystal Microbalances. Materials Research Society Symposia Proceedings, 2012, 1426, 307-311.	0.1	7
182	Subacute Pulmonary Toxicity of Copper Indium Gallium Diselenide Following Intratracheal Instillations into the Lungs of Rats. Journal of Occupational Health, 2012, 54, 187-195.	2.1	13
183	Effects of Atmospheric Pressure Dielectric Barrier Discharge Plasma Irradiation on Yeast Growth. Materials Research Society Symposia Proceedings, 2012, 1469, 86.	0.1	5
184	Investigation of chemical bonding states at interface of Zn/organic materials for analysis of early stage of inorganic/organic hybrid multi-layer formation. Thin Solid Films, 2012, 523, 15-19.	1.8	0
185	Effects of crystalline nanoparticle incorporation on growth, structure, and properties of microcrystalline silicon films deposited by plasma chemical vapor deposition. Thin Solid Films, 2012, 523, 29-33.	1.8	5
186	Control of radial density profile of nano-particles produced in reactive plasma by amplitude modulation of radio frequency discharge voltage. Thin Solid Films, 2012, 523, 76-79.	1.8	8
187	Growth Control of Dry Yeast Using Scalable Atmospheric-Pressure Dielectric Barrier Discharge Plasma Irradiation. Japanese Journal of Applied Physics, 2012, 51, 11PJ02.	1.5	13
188	The blocking effect of charge recombination by sputtered and acid-treated ZnO thin film in dye-sensitized solar cells. Journal of Photochemistry and Photobiology A: Chemistry, 2012, 248, 50-54.	3.9	18
189	Evaluation of Crystal Orientation for (K,Na)NbO\$_{3}\$ Films Using X-ray Diffraction Reciprocal Space Map and Relationship between Crystal Orientation and Piezoelectric Coefficient. Japanese Journal of Applied Physics, 2012, 51, 075502.	1.5	5
190	Sheath-to-sheath transport of dust particles in a capacitively coupled discharge. Plasma Sources Science and Technology, 2012, 21, 032001.	3.1	8
191	High quality epitaxial ZnO films grown on solid-phase crystallized buffer layers. Thin Solid Films, 2012, 520, 4674-4677.	1.8	28
192	ZnO:Al Thin Films with Buffer Layers Fabricated via Nitrogen Mediated Crystallization: Effects of N <sub>2</sub> /Ar Gas Flow Rate Ratio. Transactions of the Materials Research Society of Japan, 2012, 37, 165-168.	0.2	3
193	Effect of Nitridation of Si Nanoparticles on the Performance of Quantum-Dot Sensitized Solar Cells. Japanese Journal of Applied Physics, 2012, 51, 01AD01.	1.5	18
194	Combinatorial Deposition of Microcrystalline Silicon Films Using Multihollow Discharge Plasma Chemical Vapor Deposition. Japanese Journal of Applied Physics, 2012, 51, 01AD02.	1.5	3
195	Growth Enhancement of Radish Sprouts Induced by Low Pressure O <sub>2</sub> Radio Frequency Discharge Plasma Irradiation. Japanese Journal of Applied Physics, 2012, 51, 01AE01.	1.5	58
196	Effects of Irradiation with Ions and Photons in Ultraviolet–Vacuum Ultraviolet Regions on Nano-Surface Properties of Polymers Exposed to Plasmas. Japanese Journal of Applied Physics, 2012, 51, 01AJ02.	1.5	7
197	Improvement on the Long-Term Stability of Dye-Sensitized Solar Module by Structural Alternation. Japanese Journal of Applied Physics, 2012, 51, 10NE21.	1.5	3
198	Growth Control of Dry Yeast Using Scalable Atmospheric-Pressure Dielectric Barrier Discharge Plasma Irradiation. Japanese Journal of Applied Physics, 2012, 51, 11PJ02.	1.5	47

#	Article	IF	CITATIONS
199	Deposition of Cluster-Free B-doped Hydrogenated Amorphous Silicon Films Using SiH <sub>4</sub> +B <sub>10</sub> H <sub>14</sub> Multi-Hollow Discharge Plasma Chemical Vapor Deposition. Japanese Journal of Applied Physics, 2012, 51, 01AD03.	1.5	2
200	Generation and Surface Modification of Si nano-particles using SiH[sub 4]â^•H[sub 2] and N[sub 2] Multi-hollow Discharges and their Application to the Third Generation Photovoltaics. , 2011, , .		0
201	Impacts of Amplitude Modulation of RF Discharge Voltage on the Growth of Nanoparticles in Reactive Plasmas. Applied Physics Express, 2011, 4, 105001.	2.4	21
202	Combinatorial analyses of plasma–polymer interactions. Surface and Coatings Technology, 2011, 205, S484-S489.	4.8	12
203	Surface nitridation of silicon nanoâ€particles using double multiâ€hollow discharge plasma CVD. Physica Status Solidi C: Current Topics in Solid State Physics, 2011, 8, 3017-3020.	0.8	26
204	Hybrid sensitized solar cells using Si nanoparticles and ruthenium dye. Physica Status Solidi C: Current Topics in Solid State Physics, 2011, 8, 3021-3024.	0.8	7
205	Deposition of clusterâ€free Pâ€doped aâ€Si:H films using SiH <sub>4</sub> +PH <sub>3</sub> multiâ€hollow discharge plasma CVD. Physica Status Solidi C: Current Topics in Solid State Physics, 2011, 8, 3013-3016.	0.8	2
206	Preface: Phys. Status Solidi C 10/2011. Physica Status Solidi C: Current Topics in Solid State Physics, 2011, 8, 2975-2977.	0.8	1
207	Comparison between silicon thin films with and without incorporating crystalline silicon nanoparticles into the film. Thin Solid Films, 2011, 519, 6896-6898.	1.8	5
208	Effects of photoirradiation in UV and VUV regions during plasma exposure to polymers. Thin Solid Films, 2011, 519, 6810-6814.	1.8	18
209	Plasma processing of soft materials for development of flexible devices. Thin Solid Films, 2011, 519, 6721-6726.	1.8	14
210	Redox Characteristics of Thiol Compounds Using Radicals Produced by Water Vapor Radio Frequency Discharge. Japanese Journal of Applied Physics, 2011, 50, 08JF04.	1.5	12
211	Nano-factories in plasma: present status and outlook. Journal Physics D: Applied Physics, 2011, 44, 174038.	2.8	40
212	Highly Conducting and Very Thin ZnO:Al Films with ZnO Buffer Layer Fabricated by Solid Phase Crystallization from Amorphous Phase. Applied Physics Express, 2011, 4, 011101.	2.4	61
213	Redox Characteristics of Thiol Compounds Using Radicals Produced by Water Vapor Radio Frequency Discharge. Japanese Journal of Applied Physics, 2011, 50, 08JF04.	1.5	10
214	Redox characteristics of amino acids using low pressure water vapor RF plasma. , 2010, , .		0
215	High rate deposition of highly stable a-Si:H films using multi-hollow discharges for thin films solar cells. Surface and Coatings Technology, 2010, 205, S241-S245.	4.8	35
216	Review of pulmonary toxicity of indium compounds to animals and humans. Thin Solid Films, 2010, 518, 2934-2936.	1.8	95

#	Article	IF	CITATIONS
217	X-ray photoelectron spectroscopy for analysis of plasma–polymer interactions in Ar plasmas sustained via RF inductive coupling with low-inductance antenna units. Thin Solid Films, 2010, 518, 3555-3560.	1.8	16
218	Low-damage surface modification of polymethylmethacrylate with argon–oxygen mixture plasmas driven by multiple low-inductance antenna units. Thin Solid Films, 2010, 518, 3561-3565.	1.8	14
219	X-Ray photoelectron spectroscopy analysis of plasma–polymer interactions for development of low-damage plasma processing of soft materials. Thin Solid Films, 2010, 518, 6492-6495.	1.8	22
220	Advanced research and development for plasma processing of polymers with combinatorial plasma-process analyzer. Thin Solid Films, 2010, 518, 6320-6324.	1.8	7
221	Low-damage plasma processing of polymers for development of organic-inorganic flexible devices. Surface and Coatings Technology, 2010, 205, S355-S359.	4.8	11
222	Quantum dot-sensitized solar cells using Si nanoparticles. Transactions of the Materials Research Society of Japan, 2010, 35, 597-599.	0.2	11
223	Effects of hydrogen dilution on electron density in multi-hollow discharges with magnetic field for A-Si:H film deposition. , 2010, , .		Ο
224	Effects of Ar addition on breakdown voltage in a Si(CH <inf>3</inf> ) <inf>2</inf> (OCH <inf>3</inf> ) <inf>2</inf> RF discharge. , 2010, , .		0
225	Etching characteristics of organic low-k films interpreted by internal parameters employing a combinatorial plasma process in an inductively coupled H2/N2 plasma. Journal of Applied Physics, 2010, 107, .	2.5	20
226	Deposition profiles of microcrystalline silicon films using multi-hollow discharge plasma CVD. , 2010, , .		0
227	Photoluminescence of Si nanoparticles synthesized using multi-hollow discharge plasma CVD. , 2010, , $\cdot$		1
228	Surface loss probabilities of H and N radicals on different materials in afterglow plasmas employing H2 and N2 mixture gases. Journal of Applied Physics, 2010, 107, 103310.	2.5	17
229	Cluster-free B-doped a-Si:H films deposited using SiH <inf>4</inf> + B <inf>10</inf> H <inf>14</inf> multi-hollow discharges. , 2010, , .		Ο
230	High performance of compact radical monitoring probe in H2/N2 mixture plasma. Journal of Vacuum Science and Technology B:Nanotechnology and Microelectronics, 2010, 28, L17-L20.	1.2	4
231	Deposition of cluster-free P-doped A-Si:H films using a multi-hollow discharge plasma CVD method. , 2010, , .		Ο
232	Substrate temperature dependence of feature profile of carbon films on substrate with submicron trenches. , 2010, , .		2
233	Keynote speech I: Fluctuation control for plasma nanotechnologies. , 2010, , .		0
234	Si quantum dot-sensitized solar cells using Si nanoparticles produced by plasma CVD. , 2010, , .		1

#	Article	IF	CITATIONS
235	Effects of amplitude modulation of rf discharge voltage on growth of nano-particles in reactive plasmas. , 2010, , .		0
236	Growth stimulation of radish sprouts using discharge plasmas. , 2010, , .		2
237	Combinatorial Analysis of Plasma–Surface Interactions of Poly(ethylene terephthalate) with X-ray Photoelectron Spectroscopy. Japanese Journal of Applied Physics, 2010, 49, 08JA02.	1.5	3
238	Characterization of Dust Particles Ranging in Size from 1 nm to 10 µm Collected in the LHD. Plasma and Fusion Research, 2009, 4, 034-034.	0.7	26
239	Deposition Profile Control of Carbon Films on Patterned Substrates using a Hydrogen-assited Plasma CVD Method. Materials Research Society Symposia Proceedings, 2009, 1222, 1.	0.1	7
240	High rate deposition of cluster-suppressed amorphous silicon films deposited using a multi-hollow discharge plasma CVD. Materials Research Society Symposia Proceedings, 2009, 1210, 1.	0.1	0
241	Fabrication,Transport and Raman Studies of Pulsed Laser Deposited Al/Ga Doped PBCO Thin Films. Materials Research Society Symposia Proceedings, 2009, 1222, 1.	0.1	0
242	Plasma surface treatment of polymers with inductivity-coupled RF plasmas driven by low-inductance antenna units. Thin Solid Films, 2009, 518, 1006-1011.	1.8	26
243	Development of density-inclination plasmas for analysis of plasma nano-processes via combinatorial method. Thin Solid Films, 2009, 518, 1020-1023.	1.8	3
244	P-type sp3-bonded BN/n-type Si heterodiode solar cell fabricated by laser–plasma synchronous CVD method. Journal Physics D: Applied Physics, 2009, 42, 225107.	2.8	6
245	Combinatorial Plasma Etching Process. Applied Physics Express, 2009, 2, 096001.	2.4	15
246	Discharge power dependence of Hα intensity and electron density of Ar+H2 discharges in H-assisted plasma CVD reactor. Surface and Coatings Technology, 2008, 202, 5659-5662.	4.8	12
247	Rapid transport of nano-particles having a fractional elementary charge on average in capacitively-coupled rf discharges by amplitude-modulating discharge voltage. Faraday Discussions, 2008, 137, 127-138.	3.2	25
248	Two-Dimensional Spatial Profile of Volume Fraction of Nanoparticles Incorporated Into a-Si:H Films Deposited by Plasma CVD. IEEE Transactions on Plasma Science, 2008, 36, 888-889.	1.3	12
249	Nanoparticle coagulation in fractionally charged and charge fluctuating dusty plasmas. Physics of Plasmas, 2008, 15, .	1.9	18
250	Temperature Dependence of Dielectric Constant of Nanoparticle Composite Porous Low-kFilms Fabricated by Pulse Radio Frequency Discharge with Amplitude Modulation. Japanese Journal of Applied Physics, 2008, 47, 6875-6878.	1.5	6
251	Transport of nano-particles in capacitively coupled rf discharges without and with amplitude modulation of discharge voltage. Journal Physics D: Applied Physics, 2007, 40, 2267-2271.	2.8	32
252	Electron field emission in air at an atmospheric pressure from sp3-bonded 5Hâ€BN microcones. Journal of Applied Physics, 2007, 101, 084904.	2.5	12

#	Article	IF	CITATIONS
253	Control of Nanostructure of Plasma CVD Films for Third Generation Photovoltaics. Journal of Physics: Conference Series, 2007, 86, 012021.	0.4	2
254	Single step method to deposit Si quantum dot films using H2+SiH4 VHF discharges and electron mobility in a Si quantum dot solar cell. Surface and Coatings Technology, 2007, 201, 5468-5471.	4.8	50
255	A device for trapping nano-particles formed in processing plasmas for reduction of nano-waste. Surface and Coatings Technology, 2007, 201, 5701-5704.	4.8	5
256	Transport of Nano-particles.in Amplitude Modulated RF Discharges. Transactions of the Materials Research Society of Japan, 2007, 32, 501-504.	0.2	3
257	Properties of Nano-Crystalline Silicon Films for Top Solar Cells. , 2006, , .		0
258	Incorporation of Higher-Order Silane Radicals Into A-Si:H Films of High Stability Against Light Exposure. , 2006, , .		3
259	Plasma CVD for Producing Si Quantum Dot Films. , 2006, , .		0
260	Species responsible for Si–H2 bond formation in a-Si:H films deposited using silane high frequency discharges. Thin Solid Films, 2006, 506-507, 17-21.	1.8	17
261	Mechanism of Cu deposition from Cu(EDMDD)2 using H-assisted plasma CVD. Thin Solid Films, 2006, 506-507, 197-201.	1.8	20
262	Nano-particle formation due to interaction between H2 plasma and carbon wall. Thin Solid Films, 2006, 506-507, 656-659.	1.8	0
263	Production of crystalline Si nano-clusters using pulsed H2+SiH4 VHF discharges. Thin Solid Films, 2006, 506-507, 288-291.	1.8	29
264	Fractal growth mechanism of sp3-bonded 5H-BN microcones by plasma-assisted pulsed-laser chemical vapor deposition. Journal of Chemical Physics, 2006, 125, 084701.	3.0	7
265	Fractal growth of sp3-bonded 5H-BN microcones by plasma-assisted laser chemical vapor deposition. Journal of Applied Physics, 2006, 99, 123512.	2.5	9
266	In situ simple method for measuring size and density of nanoparticles in reactive plasmas. Journal of Applied Physics, 2006, 99, 083302.	2.5	36
267	Boron nitride microfibers grown by plasma-assisted laser chemical vapor deposition without a metal catalyst. Applied Physics Letters, 2006, 88, 151914.	3.3	8
268	Control of deposition profile of Cu for large-scale integration (LSI) interconnects by plasma chemical vapor deposition. Pure and Applied Chemistry, 2005, 77, 391-398.	1.9	16
269	Deposition of High-Quality a-Si:H by Suppressing Growth of a-Si Clusters in SiH4 Plasmas. AIP Conference Proceedings, 2005, , .	0.4	0
270	EVALUATION OF CONTRIBUTION OF HIGHER-ORDER SILANE RADICALS IN SILANE DISCHARGES TO SI-H2 BOND FORMATION IN A-SI:H FILMS. , 2005, , 79-82.		0

#	Article	IF	CITATIONS
271	Cluster-eliminating filter for depositing cluster-free a-Si:H films by plasma chemical vapor deposition. Review of Scientific Instruments, 2005, 76, 113501.	1.3	21
272	Highly Stable a-Si:H Films Deposited by Using Multi-Hollow Plasma Chemical Vapor Deposition. Japanese Journal of Applied Physics, 2005, 44, L1430-L1432.	1.5	57
273	Fabrication of Nanoparticle Composite Porous Films Having Ultralow Dielectric Constant. Japanese Journal of Applied Physics, 2005, 44, L1509-L1511.	1.5	48
274	EFFECTS OF SPUTTERING DUE TO ION IRRADIATION ON PLASMA ANISOTROPIC CVD OF CU. , 2005, , 75-78.		0
275	Anisotropic deposition of Cu in trenches by H-assisted plasma chemical vapor deposition. Journal of Vacuum Science and Technology A: Vacuum, Surfaces and Films, 2004, 22, 1903-1907.	2.1	11
276	Correlation between volume fraction of clusters incorporated into a-Si:H films and hydrogen content associated with Si–H2 bonds in the films. Journal of Vacuum Science and Technology A: Vacuum, Surfaces and Films, 2004, 22, 1536-1539.	2.1	42
277	Condensation of sp3-Bonded Boron Nitride through a Highly Nonequilibrium Fluid State. Journal of Physical Chemistry B, 2004, 108, 205-211.	2.6	9
278	Electron Field Emission from Self-Organized Micro-Emitters of sp3-Bonded 5H Boron Nitride with Very High Current Density at Low Electric Field. Journal of Physical Chemistry B, 2004, 108, 5182-5184.	2.6	22
279	The changes in particle charge distribution during rapid growth of particles in the plasma reactor. Journal of Colloid and Interface Science, 2003, 257, 195-207.	9.4	24
280	Cluster-suppressed plasma CVD for deposition of high quality a-Si:H films. Thin Solid Films, 2003, 427, 1-5.	1.8	20
281	Effects of Excitation Frequency and H2 Dilution on Cluster Generation in Silane High-Frequency Discharges. Materials Research Society Symposia Proceedings, 2003, 762, 951.	0.1	2
282	é«~効率薄膜ã,•ãfªã,³ãf³å¤é™½é›»æ±ã®ãŸã,ã®ã,¯ãf©ã,¹ã,¿å^¶å¾¡ãf—ãf©ã,ºãfžCVD. Hyomen Gijutsu/Jo	urmabof th	ne <b>S</b> urface Fin
283	Anisotropic Plasma ChemicalVapor Deposition of Copper Films in Trenches. Materials Research Society Symposia Proceedings, 2003, 766, 381.	0.1	1
284	Highly crystalline 5H-polytype of sp3-bonded boron nitride prepared by plasma-packets-assisted pulsed-laser deposition: An ultraviolet light emitter at 225 nm. Applied Physics Letters, 2002, 81, 4547-4549.	3.3	20
285	Cluster-Suppressed Plasma Chemical Vapor Deposition Method for High Quality Hydrogenated Amorphous Silicon Films. Japanese Journal of Applied Physics, 2002, 41, L168-L170.	1.5	46
286	Nucleation and subsequent growth of clusters in reactive plasmas. Plasma Sources Science and Technology, 2002, 11, A229-A233.	3.1	23
287	Anisotropic deposition of copper by H-assisted plasma chemical vapor deposition. Materials Science in Semiconductor Processing, 2002, 5, 301-304.	4.0	10
288	H-assisted plasma CVD of Cu films for interconnects in ultra-large-scale integration. Science and Technology of Advanced Materials, 2001, 2, 505-515.	6.1	20

#	Article	IF	CITATIONS
289	Cluster-less Plasma CVD Reactor and Its Application to a-Si:H Film Deposition. Materials Research Society Symposia Proceedings, 2001, 664, 561.	0.1	3
290	Formation Kinetics and Control of Dust Particles in Capacitively-Coupled Reactive Plasmas. Physica Scripta, 2001, T89, 29.	2.5	21
291	Deposition of Smooth Thin Cu Films in Deep Submicron Trench by Plasma CVD Reactor with H Atom Source. Materials Research Society Symposia Proceedings, 2000, 612, 921.	0.1	1
292	Methods of Suppressing Cluster Growth in Silane RF Discharges. Materials Research Society Symposia Proceedings, 2000, 609, 561.	0.1	0
293	Effects of Gas Temperature Gradient, Pulse Discharge Modulation, and Hydrogen Dilution on Particle Growth in Silane RF Discharges. Japanese Journal of Applied Physics, 2000, 39, 287-293.	1.5	84
294	In situ observation of nucleation and subsequent growth of clusters in silane radio frequency discharges. Applied Physics Letters, 2000, 77, 196-198.	3.3	77
295	Conformal Deposition of High-Purity Copper Using Plasma Reactor with H Atom Source. Japanese Journal of Applied Physics, 1999, 38, 4492-4495.	1.5	15
296	Plasma-enhanced metal organic chemical vapor deposition of high purity copper thin films using plasma reactor with the H atom source. Journal of Vacuum Science and Technology A: Vacuum, Surfaces and Films, 1999, 17, 726-730.	2.1	22
297	Growth of particles in cluster-size range in low pressure and low power SiH4 rf discharges. Journal of Applied Physics, 1999, 86, 3543-3549.	2.5	33
298	Effects of Gas Flow on Particle Growth in Silane RF Discharges. Japanese Journal of Applied Physics, 1999, 38, 4556-4560.	1.5	34
299	Particle Growth Kinetics in Silane RF Discharges. Japanese Journal of Applied Physics, 1999, 38, 4542-4549.	1.5	61
300	Surface reaction probabilities and kinetics of H, SiH3, Si2H5, CH3, and C2H5 during deposition of a-Si:H and a-C:H from H2, SiH4, and CH4 discharges. Journal of Vacuum Science and Technology A: Vacuum, Surfaces and Films, 1998, 16, 278-289.	2.1	219
301	Transition of Particle Growth Region in SiH4RF Discharges. Japanese Journal of Applied Physics, 1998, 37, 5757-5762.	1.5	16
302	A study on the time evolution of surface loss probability on hydrogenated amorphous silicon films in rf discharges using infrared diode-laser absorption spectroscopy. Journal Physics D: Applied Physics, 1998, 31, 776-780.	2.8	20
303	Study on growth processes of particles in germane radio frequency discharges using laser light scattering and scanning electron microscopic methods. Journal of Applied Physics, 1998, 83, 5665-5669.	2.5	29
304	Development of Photon-Counting Laser-Light-Scattering Method for Detection of Nano-Particles Formed in CVD Plasmas The Review of Laser Engineering, 1998, 26, 449-452.	0.0	33
305	Surface Reaction Kinetics of CH3in CH4RF Discharge Studied by Time-Resolved Threshold Ionization Mass Spectrometry. Japanese Journal of Applied Physics, 1997, 36, 4752-4755.	1.5	43
306	Roles ofSiH3andSiH2Radicals in Particle Growth in rf Silane Plasmas. Japanese Journal of Applied Physics, 1997, 36, 4985-4988.	1.5	39

#	Article	IF	CITATIONS
307	Simultaneousin situmeasurements of properties of particulates in rf silane plasmas using a polarizationâ€sensitive laserâ€lightâ€scattering method. Journal of Applied Physics, 1996, 79, 104-109.	2.5	94
308	Detection of particles in rf silane plasmas using photoemission method. Journal of Applied Physics, 1996, 80, 3202-3207.	2.5	47
309	Contribution of short lifetime radicals to the growth of particles in SiH4 high frequency discharges and the effects of particles on deposited films. Journal of Vacuum Science and Technology A: Vacuum, Surfaces and Films, 1996, 14, 995-1001.	2.1	50
310	Growth processes of particles in high frequency silane plasmas. Journal of Vacuum Science and Technology A: Vacuum, Surfaces and Films, 1996, 14, 540-545.	2.1	71
311	In situ polarizationâ€sensitive laserâ€lightâ€scattering method for simultaneous measurements of twoâ€dimensional spatial size and density distributions of particles in plasmas. Journal of Vacuum Science and Technology A: Vacuum, Surfaces and Films, 1996, 14, 603-607.	2.1	36
312	Diagnostics of plasma for metal - organic chemical vapour deposition of Cu and fabrication of Cu thin films using the plasma. Journal Physics D: Applied Physics, 1996, 29, 2754-2758.	2.8	12
313	Modeling of Particle Growth in RF Silane-Helium Plasma. Japanese Journal of Applied Physics, 1994, 33, 4266-4270.	1.5	5
314	Investigation of Particulate Growth Processes in RF Silane Plasmas Using Light Absorption and Scanning Electron Microscopic Methods. Japanese Journal of Applied Physics, 1994, 33, 4198-4201.	1.5	23
315	Study on Growth Processes of Subnanometer Particles in Early Phase of Silane RF Discharge. Japanese Journal of Applied Physics, 1994, 33, 4212-4215.	1.5	15
316	Growth Kinetics and Behavior of Dust Particles in Silane Plasmas. Japanese Journal of Applied Physics, 1993, 32, 3074-3080.	1.5	44
317	Potential structure in silane radioâ€frequency discharge containing particles. Applied Physics Letters, 1993, 63, 1748-1750.	3.3	8
318	Detection of Negative Ions in a Helium-Silane RF Plasma. Japanese Journal of Applied Physics, 1992, 31, L1791-L1793.	1.5	27
319	In Situ Observation of Growing Process of Particles in Silane Plasmas and Their Effects on Amorphous Silicon Deposition. Materials Research Society Symposia Proceedings, 1991, 235, 763.	0.1	Ο
320	In Situ Observation of Growing Process of Particles in Silane Plasmas and Their Effects on Amorphous Silicon Deposition. Materials Research Society Symposia Proceedings, 1991, 236, 301.	0.1	3
321	In SituObservation of Particle Behavior in rf Silane Plasmas. Japanese Journal of Applied Physics, 1991, 30, 1887-1892.	1.5	35
322	Reincrease in Electron Density in the Current-Decaying Phase of Pulsed-Discharge of Argon-Hydrogen Mixture. Japanese Journal of Applied Physics, 1988, 27, 1469-1476.	1.5	0
323	On Shifting of Plowed Plasma to Back of Current Sheath in Implosion Phase of Theta-Pinch. Japanese Journal of Applied Physics, 1987, 26, 1334-1341.	1.5	2
324	Generation of Magnetic Islands Caused by Periodical Nonuniformity of Axial Magnetic Field for FRC Formation Phase. Japanese Journal of Applied Physics, 1987, 26, L1040-L1042.	1.5	1

#	Article	IF	CITATIONS
325	Generation of a Large Swelling in the Spatial Magnetic Field Profile near the Coil Axis of a Theta Pinch. Japanese Journal of Applied Physics, 1987, 26, 1727-1732.	1.5	1
326	Study on Electron Density Dependence of Metastable Ar+Density in Pulsed-Discharge Plasma by Using LIF Method. Japanese Journal of Applied Physics, 1987, 26, 184-185.	1.5	1
327	On Applicability of Laser-Induced Fluorescence from the Metastable State of Argon Ions to Ion Density Measurements. Japanese Journal of Applied Physics, 1986, 25, 932-933.	1.5	2
328	Dependence of Evolution of Field Reconnection at Coil End Region on Mirror Field in FRC Formation Stage. Japanese Journal of Applied Physics, 1986, 25, 762-763.	1.5	2
329	Nanostructure Control of Si and Ge Quantum Dots Based Solar Cells Using Plasma Processes. Materials Science Forum, 0, 783-786, 2022-2027.	0.3	2
330	Photoluminescence of (ZnO) <sub>0.82</sub> (InN) <sub>0.18</sub> Films: Incident Light Angle Dependence. Materials Science Forum, 0, 941, 2099-2103.	0.3	3
331	Effects of Activated Carbon Counter Electrode on Bifacial Dye Sensitized Solar Cells (DSSCs). Materials Science Forum, 0, 1016, 863-868.	0.3	3
332	Synergetic effect of a polymer and metalloid composite on the electrocatalytic improvement of dye-sensitized solar cells. New Journal of Chemistry, 0, , .	2.8	0
333	Performance Characteristics of Bifacial Dye-Sensitized Solar Cells with a V-Shaped Low-Concentrating Light System. ACS Applied Energy Materials, 0, , .	5.1	2
334	The Effects of Spin-Coating Rate on Surface Roughness, Thickness, and Electrochemical Properties of a Pt Polymer Counter Electrode. Advanced Engineering Forum, 0, 45, 1-13.	0.3	0
335	Performance comparison of nitrile-based liquid electrolytes on bifacial dye-sensitized solar cells under low-concentrated light. MRS Advances, 0, , 1.	0.9	0
336	Raman spectral analysis of the as-deposited a-C:H films prepared by CH4 + Ar plasma CVD. MRS Advanc 0, , .	es <sub>0.9</sub>	0